Supporting Information for

Delivery of Gefitinib in synergism with Thymoquinone via Transferrin Conjugated Nanoparticle Sensitizes Gefitinib Resistant Non-Small Cell Lung Carcinoma to Control Metastasis and Stemness

Priyanka Upadhyay[1], Avijit Ghosh[1], Arijita Basu[2], P. A. Pranati[1], Payal Gupta[3], Shaswati Das[1], Sushmita Sarker[1], Mousumi Bhattacharjee[1], Saurav Bhattacharya[1], Swatilekha Ghosh[4], Sreya Chattopadhyay[3], Arghya Adhikary[1]*

[1]Center for Research in Nanoscience and Nanotechnology, Technology Campus, University of Calcutta, JD-2, Sector-III, Salt Lake, Kolkata-700106, West Bengal, India.

[2]Department of Polymer Science and Technology, University of Calcutta, 92 Acharya Prafulla Chandra Road, Kolkata-700009, West Bengal, India.

[3]Department of Physiology, University of Calcutta, 92 Acharya Prafulla Chandra Road, Kolkata-700009, West Bengal, India.

[4]Amity Institute of Biotechnology, Amity University, Rajarhat, New Town, Kolkata-700156, West Bengal, India.

*To whom correspondence should be addressed: Dr. Arghya Adhikary. Centre for Research in Nanoscience and Nanotechnology, University of Calcutta, JD-2, Sector-III, Salt Lake, Kolkata-700106, West Bengal, India. Tel: +91-9830428550. E-mail: adhikaryarghya@gmail.com.

Figure S-1 (Supporting Information): FT-IR spectra of NP-dual-3

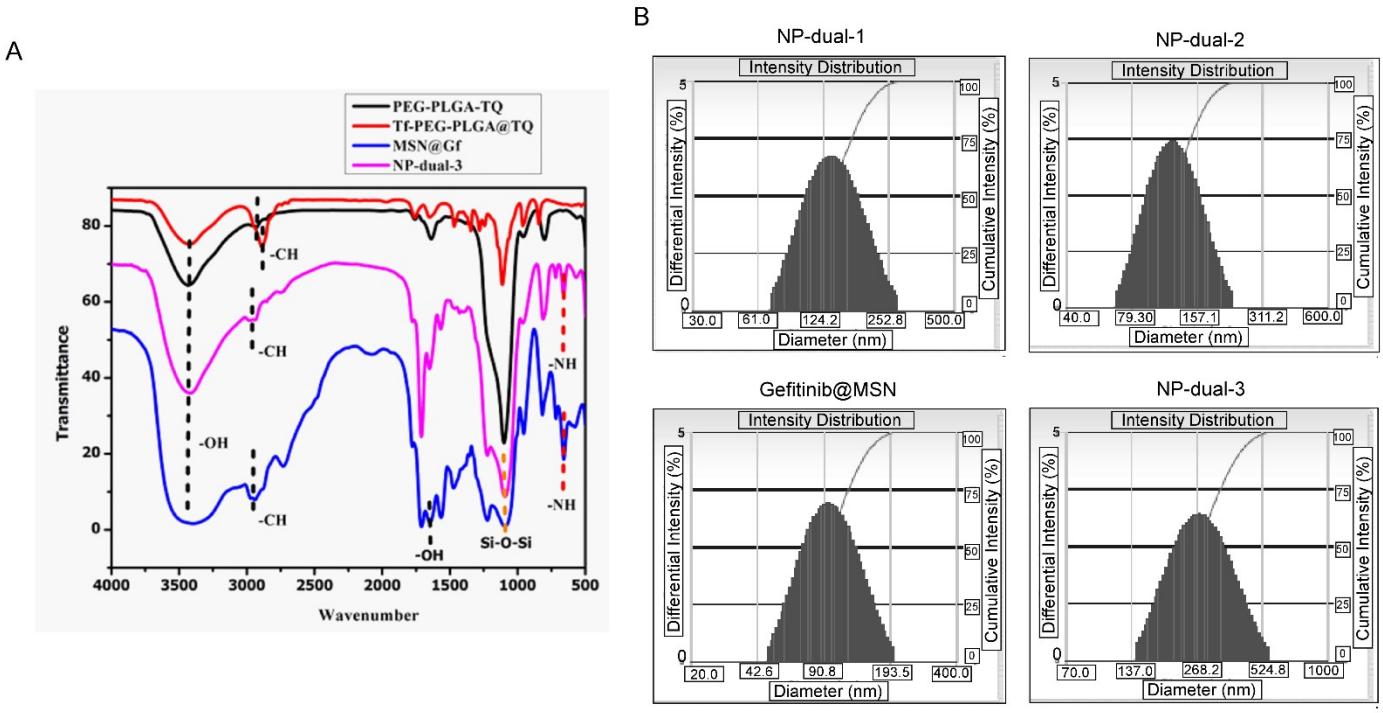

Fourier Transform Infrared Spectroscopy: FT-IR experiments were carried out to investigate the surface characteristic of target nanoparticle. Figure 2 illustrates the FT-IR spectra of gefitinib loaded MSN and PLGA encapsulated thymoquinone. The peaks at 3445 and at 1645 cm−1 showed the presence of surface -OH groups in Gefitinib loaded MSN. The strong band at 1102 cm−1 corresponds to Si–O–Si groups. On the other hand, PLGA encapsulated thymoquinone showed characteristic bands at 3444 cm−1, 1750 cm−1, and 1104 cm−1 respectively. After conjugation of transferrin, new bands at 1635 cm−1 and 2900 cm−1 were observed which are characteristic of transferrin moiety. Finally, attachment of these two nanoparticles produced target NP-dual-3 which showed strong band at 3438 cm−1, 2945 cm−1, 1634 cm−1 and 1550 cm−1. Therefore, it could be assumed that successful conjugation between two nanoparticles was achieved to obtain target combination nanoparticle.

Table S-1 (Supporting Information) **Physicochemical properties of different nanoparticles**

Name of the nanoparticle	**%EE[a] (W/W)**	**%DL[a] (W/W)**	**%Yield [c]**	**Size[d] (in nm) DLS**	**Zeta Potential(mV)**
NP-dual-1	72± 1.7	15.15± 1.2	79± 0.7	120 nm	-20
NP-dual-2	75± 1.6	15.9± 0.2	78± 0.5	140 nm	-26
NP-dual-3	85± 1.3	18.8± 1.3	75± 1.2	220 nm	-16

[a] (%) Encapsulation Efficiency (EE) = (Total amount of drugs added-Free drug)/Total amount of drug× 100

(Drugs= Thymoquinone + Gefitinib)

[b] (%)Yield = (Mass of nanoparticle obtained/Total weight of drug & polymer) × 100

[c] (%) Drug loading (DL) = (Total entrapped drug / Total nanoparticle weight) × 100

Figure S-2 (Supporting Information): **Combinatorial therapy of NP-dual-3 produced ROS in NSCLC.**

Figure S-3 (Supporting Information): **Upregulation of miR-21 targets smad7; TGF-β1 mediated EMT in NSCLC**

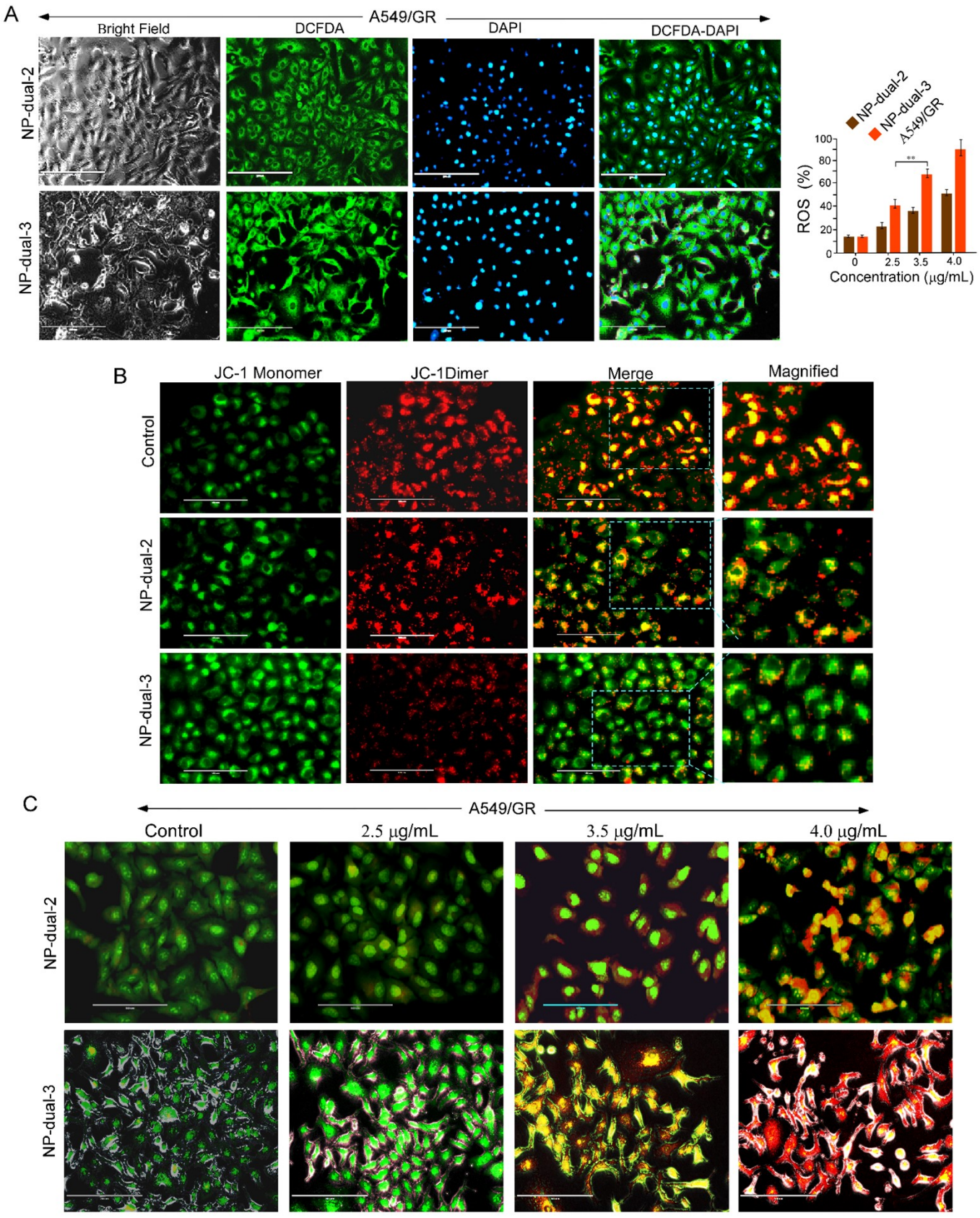
A
A549/GR
Bright Field
DCFDA
DAPI
DCFDA-DAPI
NP-dual-2
NP-dual-3
NP-dual-2
NP-dual-3
A549/GR
ROS (%)
100
80
60
40
20
0
**
0
2.5
3.5
4.0
Concentration (μg/mL)
B
JC-1 Monomer
JC-1Dimer
Merge
Magnified
Control
NP-dual-2
NP-dual-3
C
A549/GR
Control
2.5 μg/mL
3.5 μg/mL
4.0 μg/mL
NP-dual-2
NP-dual-3

Figure S-2. Examination of cellular toxicity through fluorescence imaging. (A) ROS generation depiction in NP-dual-2 (upper panel)/ NP-Dual-3 (lower panel) treated A549/GR cells & graphical representation of increase in percentage ROS generation against drug concentration (B) The treated A549 cells were stained with JC1 dye and analyzed under fluorescent microscope for changes in membrane potential with respect to untreated cells. (C) A549/GR cells were treated with different nanoparticles and stained with AO/EtBr to study cell death. The scale bar was set at 200μm.

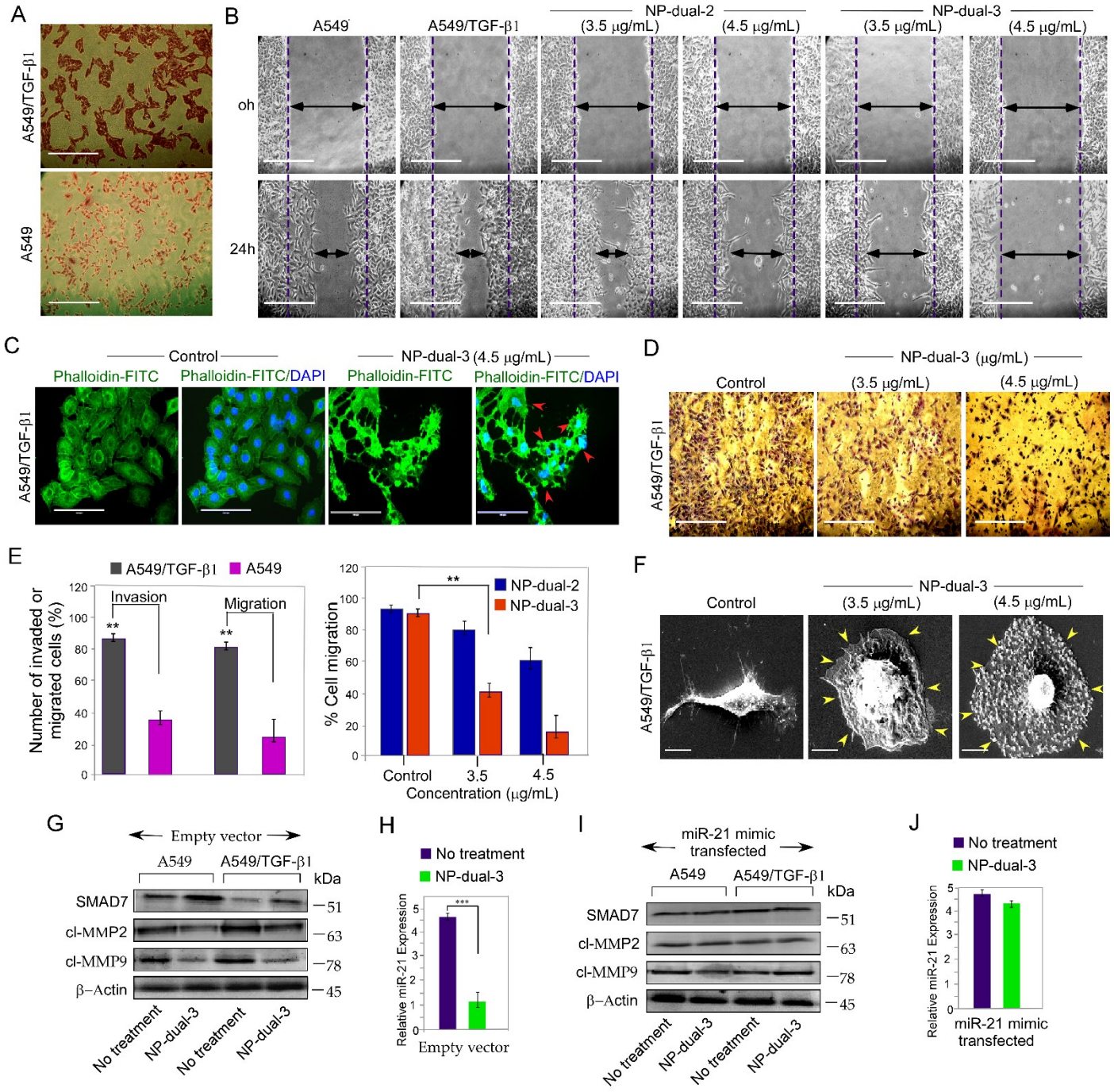

Figure S-3. NP-dual-3 attenuates TGF-β1 induced EMT in NSCLC. (A) Phase contrast images of H & E stained-A549 and A549/GR cells showing distinguished morphological features. The scale bar was set at 200μm. (B) Phase-contrast pictures of bi-directional wound healing assay showing pattern of migration in A549 and A549/ TGF-β1 cells on treatment with or without NP-dual-3 or NP-dual-3 at 0 h (upper panel) to 24 h (lower panel). The scale bar was set at 200μm. (C) A549/TGF-β1 cells were treated with NP-dual-3 for overnight and allowed for phalloidine staining to study the status of cytoskeleton configuration as compared to control cells. The fluorescent images showed that the structure of cytoskeleton was abruptly distorted left with very less number of F-actin in the impact of nanoparticle treatment unlike the control cells, bearing compact and organized cellular backbone. (D) Transwell migration assay signified that maximum number of untreated A549/ TGF-β1 cells have migrated to undersurface unlike the treated cells. The scale bar was set at 200μm. (E) The bar graph showing the comparative profiling of A549 and A549/ TGF-β1 cells for their invasion and migration ability. The migration efficiency of A549/ TGF-β1 after treatment with different nanoparticle at various concentration was presented by bar graph pattern, derived from wound healing assay. (F) The Bio-SEM pictures of differently treated A549/ TGF-β1 cells showing irregular cell-morphology with distorted cytoskeleton coupled with membrane blabbing in treated cells as compared to control cells, bearing increased number of intact protrusions. The scale bar was set at 50μm. (G) A549 and A549/ TGF-β1 cells were transfected with miR-21 mimic or empty vector. The cells of both transfected and empty vector-transfected batch were treated with NP-dual-3 or left untreated and subjected to different analysis. Western blot analysis showed that NP-dual-3 treatment induced upregulation of SMAD7 and downregulation of cl-MMP2 and cl-MMP9 in A549 or A549/ TGF-β1 cells. (I) However, in similar set of experiment overexpression of miR-21 neutralizes the therapeutic effect of NP-dual-3 in restriction of TGF-β1 induced EMT in A549/ TGF-β1. Here, β-actin acted as internal control. (H, J) The qRT-PCR analysis revealed the expression pattern of miR-21 in transfected or empty vector-transfected batch of A549/ TGF-β1 cells, either treated or left untreated with NP-dual-3. Values are mean ±SEM of three independent experiments in each case or representative of typical experiment. ***P<0.001.

In vitro drug release

In order to evaluate the TQ/Gf release pattern from each nanoparticles *in-vitro* drug release was examined. Briefly, 40 mg of NP-Dual-1/ NP-Dual-2/ NP-Dual-3 were dispersed in 5ml phosphate buffer with pH7.4 and pH5.2 respectively. Then these solutions were transferred inside a dialysis membrane whose MWCO is 2KDa (Sigma, USA). The membrane was placed against 100ml of respective phosphate buffer in a beaker at a stirring rate of 150rpm at 37°C. At various time intervals, 3mL of the dialyzed buffer was withdrawn and the absorbance at ~257 nm for TQ and 332/346 nm for Gf was measured to determine the quantity/percentage of the total drug released and 3mL of fresh phosphate buffer was added to the dialysis solution to maintain sink volume.